Available online at www.sciencedirect.com
ScienceDirect
Catalysis Today 129 (2007) 102–109
CATALYSIS TODAY
www.elsevier.com/locate/cattod

Screening of different zeolite-based catalysts for gas-phase selective photooxidation of propan-2-ol

M.A. Aramendía, J.C. Colmenares, S. López-Fernández, A. Marinas *, J.M. Marinas, F.J. Urbano

Departamento de Química Orgánica, Universidad de Córdoba, Edf, Marie Curie, Campus Universitario de Rabanales, 14014 Córdoba, Spain

Abstract

In the present piece of research photocatalytic activity of TiO_2 and V_2O_5 (as measured for gas-phase selective photoxidation of propan-2-ol) is substantially improved through their sol–gel synthesis on USY zeolites. The decrease in the crystallite size of TiO_2 (anatase) and V_2O_5 thus exhibiting the so-called quantum size effect (as determined by XRD and UV–vis spectroscopies, respectively) is to account for that. In the case of vanadium, the use of zeolites means a decrease in selectivity to acetone whereas no noticeable change is observed for titanium. Subsequent photodeposition of platinum on the Ti- and V-containing zeolites results in a sharp increase in molar conversion, low or negligible deactivation with a time-on-stream of 5 h and significant increase in selectivity to acetone which was in the range 90–96%.

Keywords: Propan-2-ol; Photocatalysis; Selective photooxidation; Titania; Vanadia; Zeolite-based photocatalysis; USY; Platinum-doped systems; Silver-doped systems; Quantum-size effect

1. Introduction

The main application of heterogeneous photocatalysis (at least as far as the number of the publications on the topic is concerned) is degradation of pollutants present in waters through complete mineralization [1–3]. One could think of the possibility of selectively oxidizing the pollutant to a non-toxic high-valued chemical which would be even more interesting though, unfortunately, it is not possible in aqueous media. There are some examples in the literature of selective adsorption of a chemical making use of the shape-selectivity (zeolites) [4] or the so-called adsorb-and-shuttle concept [5,6]. These approaches allow selective adsorption though once adsorbed, the chemical will tend to be mineralized. Nevertheless, selective oxidations can be performed in non-aqueous media. Therefore, gas-phase selective oxidation of propan-2-ol to acetone is often used as a model reaction for characterization of photocatalytic activity [7–9].

As regards the photocatalyst itself, titania is by far the most-widely used system, but it has some drawbacks such as the absorption in the UV-region or the low surface area. In this sense, as pointed out by Corma and García [10], some of the advantages of using zeolites in photocatalysis are as follows:

(i) High surface area, thus enabling high adsorption of chemicals to be photo-oxidised/reduced.
(ii) Transparency to UV–vis radiation above 240 nm thus allowing a certain penetration of the exciting light into the powder which can be useful in order to allow exciting light to reach a photoactive guest.
(iii) Possibility to vary the chemical composition of framework and out-of-framework position in a large extent, thus rendering these molecular sieves photoactive (e.g. introducing Ti or V atoms).
(iv) Possibility to modulate both the micropolarity of the zeolite interior and the size of the channels.

Two of the most common methods of preparation of titania into zeolites are ion exchange from titanyl solutions [11,12] or hydrolysis of titanium alkoxide [13,14].

* Corresponding author. Tel.: +34 957218622; fax: +34 957212066.
E-mail addresses: alberto.marinas@uco.es (A. Marinas), fj.urbano@uco.es (F.J. Urbano).

0920-5861/$ – see front matter © 2007 Elsevier B.V. All rights reserved.
doi:10.1016/j.cattod.2007.09.005

The relatively high electron–hole recombination rate of TiO_2 constitutes an additional drawback since it is detrimental to its activity. In this sense, doping with metals could make a double effect: (i) firstly, it could reduce the band gap energy, thus shifting the absorption band to the visible region and (ii) secondly, metals could provoke a decrease in electron–hole recombination rate, acting as electron traps.

The present piece of research is aimed at exploring the possibility of improving the photocatalytic activity of titania, vanadia and zinc oxide through their sol–gel synthesis on USY zeolites and the subsequent doping with Pt or Ag.

2. Experimental

2.1. Synthesis of Ti, V and Zn-containing zeolites

Zeolite-based photocatalysts were synthesized through the sol–gel method starting from titanium isopropoxide [$Ti(OCH(CH_3)_2)_4$,] vanadyl acetylacetonate [$VO(acac)_2$] and zinc acetylacetonate [$Zn(acac)_2$] which were incorporated, in a nominal content of 2 mmol/g of catalyst, on USY (Si/Al = 62 and 4.7) zeolites.

In order to obtain titanium-containing systems, 10 g of zeolite previously treated at 400 °C in air flow for 4 h were introduced in a 250 mL round-bottom flask together with 60 mL of propan-2-ol and 6.14 mL titanium isopropoxide. The mixture was heated at ca. 90 °C (propan-2-ol reflux) for 14 h. Then, a solution of 322.5 mg dipicolinic acid in a mixture of 20 mL propan-2-ol and 2.5 mL water was added in order to favor formation of the gel and the mixture was kept under reflux for two more hours. The solid was then vacuum-filtered and washed with 10 mL of propan-2-ol three times. Finally, the system was calcined at 550 °C for 4 h in static air.

Incorporation of zinc and vanadium into zeolites was carried out in a similar way as described for titanium-systems but using 2.5 mL of 6.7 M ammonia solution as the precipitation agent instead of the dipicolinic acid mixture. Moreover, vanadyl acetylacetonate had to be previously dissolved in 2 mL 30% HNO_3.

For comparative purposes, pure TiO_2, ZnO and V_2O_5 were also obtained by the same sol–gel process as described above.

All chemicals were obtained from Aldrich. Zeolites were purchased from Zeolyst Int. (CBV300 and CBV780). Prior to its use, CBV300 was calcined at 550 °C for 4 h in static air in order to convert it to its acidic form.

The nomenclature of the systems include the zeolite type (USY), together with a prefix indicating the atom (Ti, V or Zn) incorporated into the zeolite and a suffix corresponding to the Si/Al ratio as determined by ICP-MS. Therefore, for instance, Ti-USY62 refers to the USY zeolite with Si/Al = 62 into which titanium has been incorporated.

2.2. Further incorporation of platinum and silver

The most active systems containing V and Ti were then selected to incorporate Ag and Pt using silver or platinum (II) acetylacetonates (Aldrich) as the corresponding precursors. Incorporation was performed either by impregnation or photodeposition.

2.2.1. Impregnation method

1.5 g of zeolite-based photocatalyst are introduced in a round-bottom flask together with the appropriate amount of the Ag or Pt precursor as to have a nominal (Pt or Ag)/(Ti or V) atomic ratio of 0.1 dissolved in 400 mL propan-2-ol. The vanadium and titanium content in zeolites had been previously determined by inductively coupled plasma-mass spectrometry (ICP-MS). The mixture is submitted to vigorous stirring while propan-2-ol is distilled. The solid is then vacuum-filtered and washed three times with volumes of 15 mL of propan-2-ol. Finally, the system is calcined in static air at 550 °C for 4 h, thus yielding the solids belonging to the "I" series (standing for Impregnation).

2.2.2. Photodeposition method

Photodeposition of Pt and Ag was carried out in a Pyrex cylindrical double-walled immersion well reactor (23 cm long, 5 cm internal diameter, with a total volume of ca. 450 cm^3) open to air starting from 1.5 g of zeolite and the Pt and Ag precursor dissolved in 400 mL propan-2-ol. Irradiation of the reaction solutions was carried out by using a medium pressure 125 W Hg lamp (λ_{max} = 365 nm) supplied by Photochemical Reactors Ltd. (Model 3010). Lamp output was calculated to be ca. 1.5×10^{-3} einstein/s (potassium ferrioxalate actinometry). Water used for cooling was thermostated at 20 °C. Constant agitation of the suspension was insured by a magnetic stirrer placed at the reactor base. Further details on the experimental device are given elsewhere [15]. Irradiation time was 2 h. The systems were vacuum-filtered, washed with propan-2-ol and calcined at 550 °C for 4 h, thus yielding the solids belonging to the "P" series (standing for Photodeposition).

The nomenclature of the systems includes a prefix referring to the incorporation method (impregnation or photodeposition) and the metal incorporated (Ag or Pt). Therefore, for instance, PPt-Ti-USY62 refers to a USY zeolite with a Si/Al ratio equal to 62, to which titanium had been incorporated by the sol–gel method and platinum was then added by photodeposition.

2.3. Characterization

Elemental analyses were carried out by the staff at the Central Service for the support of research (SCAI) at the University of Córdoba. Measurement was made on a ICP-MS ELAN-DRC-e (Perkin Elmer), after dissolution of the samples in a H_2SO_4:HF:H_2O (1:1:1) mixture. Atomic spectroscopy standards from Inorganic Ventures Inc. (ISO-CAL-28, ISO-CAL-29, ISO-CAL-30 and CGAU1-1) were used for calibration.

As far as EDX analyses are concerned, they were performed on a JEOL JSM-6300 SEM apparatus operating at an accelerating voltage of 20 keV with a resolution of 65 eV. EDX values corresponded to the average value of four measurements carried out at different areas of the solid with an amplification of 5000×.

The textural properties of solids (specific surface area, pore volume and mean pore radius) were determined from nitrogen adsorption–desorption isotherms at liquid nitrogen temperature by using a Micromeritics ASAP-2010 instrument. Surface areas were calculated by the BET method, while pore distributions were determined by the BJH method. Prior to measurements, all samples were degassed at 200 °C to 0.1 Pa. Moreover, as recommended elsewhere [16] for adsorption isotherms, nitrogen gas was dosed onto the samples in increments of 3 mL/g of solid for data points below 0.03 P/P_0.

X-ray analyses of solids were carried out using a Siemens D-5000 diffractometer provided with an automatic control and data acquisition system (DACO-MP). The patterns were run with nickel-filtered copper radiation (λ = 1.5406 A) at 40 kV and 30 mA; the diffraction angle 2θ was scanned at a rate of 2° min^{-1}. The average crystallite size of anatase in pure TiO_2 and V_2O_5 was determined according to the Scherrer equation using the full-width at half maximum (FWHM) of the peaks corresponding to 1 0 1 and 0 0 1 reflections, respectively, and taking into account the instrument broadening.

FT-Raman spectra were obtained on a Perkin-Elmer 2000 NIR FT-Raman system with a diode pumped Nd:YAG laser (9394.69 cm^{-1}). It was operated at a resolution of 4 cm^{-1} throughout the 3600–200 cm^{-1} range to gather 64 scans. Laser power was set at 300 mW.

Diffuse reflectance UV–vis spectra were performed on a Cary 1E (Varian) instrument, using barium sulphate as reference material. Band gap values were obtained from the plot of the modified Kubelka–Munk function $[F(R_\infty)E]^{1/2}$ versus the energy of the absorbed light E. [17,18]. Regarding absorption threshold, it was determined according to the formula [19]:

$$\lambda = \frac{hc}{E_{gap}} = \frac{1240}{E_{gap}}$$

FT-IR spectra were recorded over a wavenumber range 400–4000 cm^{-1} on a Bomen MB-100 FT-IR spectrophotometer. The pellets were prepared by mixing the powdered solid with KBr in a 5:95 (w/w) ratio.

2.4. Photocatalytic experiments

In photocatalytic experiments, 20 mL min^{-1} of a He:O_2 (90:10, v/v) mixture previously bubbled through propan-2-ol at 0 °C was allowed into the photocatalytic reactor, in which 30 mg of catalyst (previously heated for 8 h at 400 °C in N_2 flow) had been placed. The fix bed of the catalyst is in contact with the gas flow. UV light (UV Spotlight source Lightning-cure™ L8022, Hamamatsu, maximum emission at 365 nm) was focalized on the sample compartment through an optic fiber. Reactor was thermostated by circulating water at 20 °C through the external wall. Radiant flux in the catalyst compartment was measured to be 1.1 W cm^{-2} (Hamamatsu UV-meter, C6080-03 Model). Reactor was on-line connected to a HP6890 chromatograph equipped with a six-way valve, a HP-PLOTU column (30 m long, 0.53 mm i.d., 20 μm film thickness) and a Ni methanator (Agilent Part Number G2747A) which allowed us to determine the percentage of CO_2 resulting from mineralization of propan-2-ol. Further details on the photocatalytic device are given elsewhere [20].

3. Results and discussion

3.1. First screening and characterization of the most active systems

Results found for the systems of vanadium and titanium incorporated to USY zeolites in the gas-phase selective oxidation of propan-2-ol are given in Fig. 1. For the sake of comparison, those achieved with the corresponding pure vanadia and titania systems have also been included. Zn-containing systems are not represented since they gave molar conversions below 1%. Therefore, such systems were already ruled out at the early stages of the screening.

For all the systems studied in the present work, the main products detected were acetone, acetaldehyde, propene and carbon dioxide with traces of methanol and acetic acid. The suggested mechanisms for their obtaining are as follows:

$$CH_3CHOHCH_3 \rightarrow CH_3CH{=}CH_2 + H_2O \quad \text{(dehydration)}$$

$$CH_3CHOHCH_3 + O_2 \rightarrow CH_3COCH_3 + 2OH^\bullet$$
(selective oxidation to acetone)

$$CH_3CHOHCH_3 + 2OH^\bullet \rightarrow CH_3COH + CH_3OH + H_2O$$
(oxidative cleavage)

Xu and Raftery [21] studied photocatalytic oxidation of 2-propanol on TiO_2 by in situ solid-state NMR reporting two adsorbed 2-propanol species accounting for two parallel routes for 2-propanol photocatalytic oxidation. The first route occurred with the formation of acetone from the H-bonded 2-propanol species followed by aldol condensation of acetone to form mesityl oxide. In our case, diaceton-alcohol (which on dehydration would yield mesityl oxide) was also observed by mass spectrometry. The second route reported by the authors implies the relatively rapid and complete oxidation of 2-propoxide to CO_2. Moreover, CO_2 could result from complete mineralization of any of the above-mentioned organic compounds.

Finally, the fact that acetaldehyde is obtained in much higher yield than methanol seems to suggest the existence of any other routes for its obtaining. Some authors have suggested that acetaldehyde can be obtained through fragmentation of mesityl oxide coming from acetone condensation [21]. Alternatively, acetaldehyde could come from propene oxidation. Oxidation of acetaldehyde would result in acetic acid formation. In any case, the reaction mechanism requires further studies.

Results shown in Fig. 1 are represented in terms of initial (t = 0 h) and final (time-on-stream of 5 h) molar conversion and final selectivity to acetone and CO_2. Some features concerning characterization of the systems are summarized in Table 1.

From Fig. 1 it is clear that the use of zeolites leads to a substantial increase in activity which is especially considerable

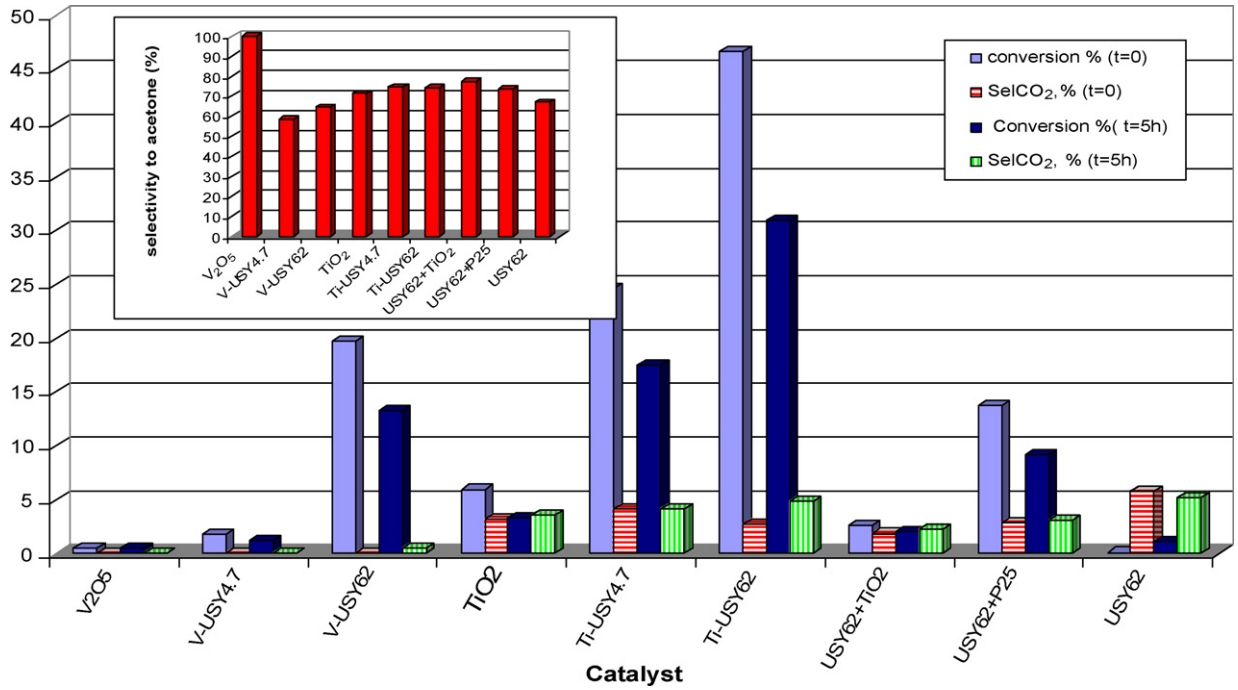

Fig. 1. Results obtained for the gas-phase selective photooxidation of propan-2-ol with the vanadium and titanium-based systems synthesized in the present work. For the sake of comparison, results achieved with USY62 and physical mixtures of such a zeolite with either commercial (Degussa P25) or our pure TiO_2 have also been included.

for those systems with the higher Si/Al ratio. The greater extent to which Ti and V have been incorporated to USY62 as compared to USY4.7 together with the higher surface area (see Table 1) could account for that. In the case of vanadium-containing systems, the utilization of zeolites means a noticeable decrease of selectivity to acetone whereas no change is observed for titanium-containing ones, their selectivity to acetone remaining in the 70–75% range (see the inset in Fig. 1).

Finally, it is noteworthy that all zeolitic materials present a relatively high deactivation (ca. 30%).

One could think that, as data are expressed for the same catalyst weight (30 mg), the higher conversion of zeolitic materials as compared to pure oxides is just the result of their much higher surface area. Therefore, for instance, Ti-USY62 has a BET surface area of 589 m^2/g whereas TiO_2 only has 6 m^2/g. In order to rule out such a possibility, once titanium

Table 1
Some features concerning characterization of the systems synthesized in the present work

Catalyst	UV–vis		ICP-MS			EDX	N_2 isotherms
	Band gap (eV)	Absorption threshold (nm)	Ti, V or Zn/g catalyst (mmol)	Metal/(Ti or V) (at.%)	Metal wt.% in the solid	Metal/(Ti or V) (%)	S_{BET} (m^2/g)
1. USY62	–	–	–	–	–	–	691
2. USY4.7	–	–	–	–	–	–	663
3. TiO_2	3.07	404	12.5	–	–	–	6
4. Ti-USY62	3.29	377	1.8	–	–	–	589
5. Ti-USY4.7	3.30	376	1.4	–	–	–	476
6. V_2O_5	2.16	574	11.0	–	–	–	5
7. V-USY62	2.23	556	1.5	–	–	–	427
8. V-USY4.7	2.17	571	0.9	–	–	–	22
9. ZnO	3.22	385	12.3	–	–	–	9
10. Zn-USY62	3.24	382	1.5	–	–	–	562
11. Zn-USY4.7	3.24	382	1.1	–	–	–	64
12. PPt-Ti-USY62	3.24	382	1.5	2.5	0.71	6.5	580
13. IPt-Ti-USY62	3.41	364	1.5	0.1	0.04	4.6	609
14. PPt-V-USY62	2.08	596	0.7	0.8	0.11	11.6	437
15. IPt-V-USY62	2.05	605	0.5	0.1	0.01	1.8	477
16. PAg-Ti-USY62	3.29	377	1.5	9.7	1.57	10.3	565
17. IAg-Ti-USY62	3.35	370	1.5	11.5	1.90	14.8	581
18. PAg-V-USY62	2.07	599	0.9	36.8	3.40	41.5	533
19. IAg-V-USY62	2.06	602	0.6	30.3	1.92	31.3	533

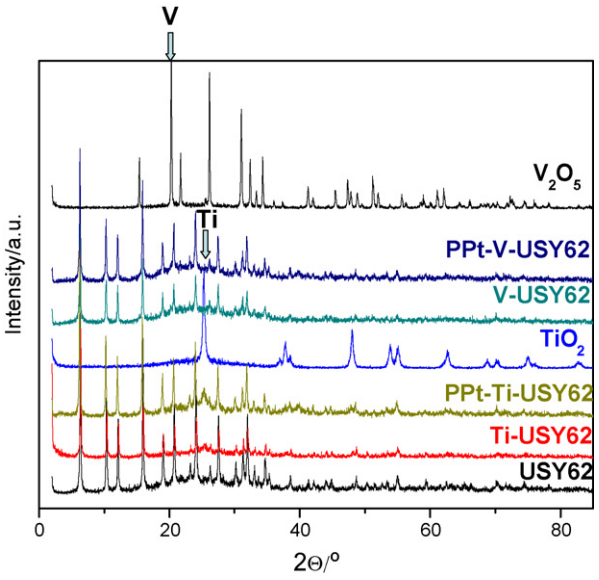

Fig. 2. XRD spectra of some systems synthesized in the present work. Vertical arrows on V_2O_5 and TiO_2 spectra indicate their 0 0 1 and 1 0 1 reflections, respectively.

content in zeolites had been determined by ICP-MS (see Table 1), an experiment on a physical mixture of USY62 and TiO_2 (at the same Ti/zeolite ratio) was performed. As can be seen in Fig. 1, molar conversion thus achieved was significant lower than the one obtained with Ti-USY62 (2.1% and 31.0%, respectively, after 5 h). A physical mixture of Degussa P25 (a well-known highly active photocatalyst) and USY62 did neither give as good results as Ti-USY62, its molar conversion for $t = 5$ h being 9.2%.

Results obtained in this preliminary screening for the different systems prompted us to choose Ti-USY62 and V-USY62 zeolites for further modification through the doping with platinum and silver.

Such zeolite-based photocatalysts were firstly fully characterized in order to search for the reason for their high activity as compared to pure oxides. In this sense, a crucial question to answer was the way titanium and vanadium had been incorporated into the zeolite. Therefore, XRD (Fig. 2), FT-Raman and FT-IR spectroscopies (Fig. 3) were used.

As far as Ti-USY62 is concerned, XRD spectrum (Fig. 2) hardly show bands of TiO_2 which suggest that either the content in such oxide is very low or its crystal size is quite small. ICP-MS results (Table 1) allow us to rule out the first possibility since titanium weight percentage in Ti-USY62 is ca. 8.5% (14% expressed as titania). On the other hand, pure TiO_2 was determined to consist of 100% anatase particles with an average cristal size of 20 nm (as determined from 1 0 1 reflection at $2\Theta = 25.30°$). The presence of 100% anatase was confirmed by FT-Raman spectroscopy. Therefore, TiO_2 Raman spectrum (Fig. 3A) exhibits theree main peaks centered at ca. 399, 518 and 640 cm^{-1}, attributed to fundamental vibrational modes of anatase B1g, A1g + B1g and Eg, respectively [22]. In the case of Ti-USY62, B1g and Eg fundamental vibrational modes of anatase are also present whereas the one corresponding to A1g + B1g mode probably overlaps with one band already present in USY62 at ca. 520 cm^{-1}. These results, together with the above-mentioned comments on XRD spectra, suggest that titanium is present in zeolites as small crystallites of anatase.

FT-IR spectra of USY62 and Ti-USY62 are depicted in Fig. 3B. No significant increase in the shoulder appearing at ca. 950–960 cm^{-1} is observed on the introduction of titanium into the zeolite. Since Si–O–Ti vibrations are reported to appear in such a region [23,24], these results seem to suggest that titanium has not been incorporated into the zeolitic structure. Instead, small anatase crystallites were deposited on the USY zeolite.

UV–vis reflectance spectra of TiO_2 and Ti-USY62 are represented in Fig. 4A. As can be seen, the formation of TiO_2 on the USY zeolite results in a blue-shift in the absorption

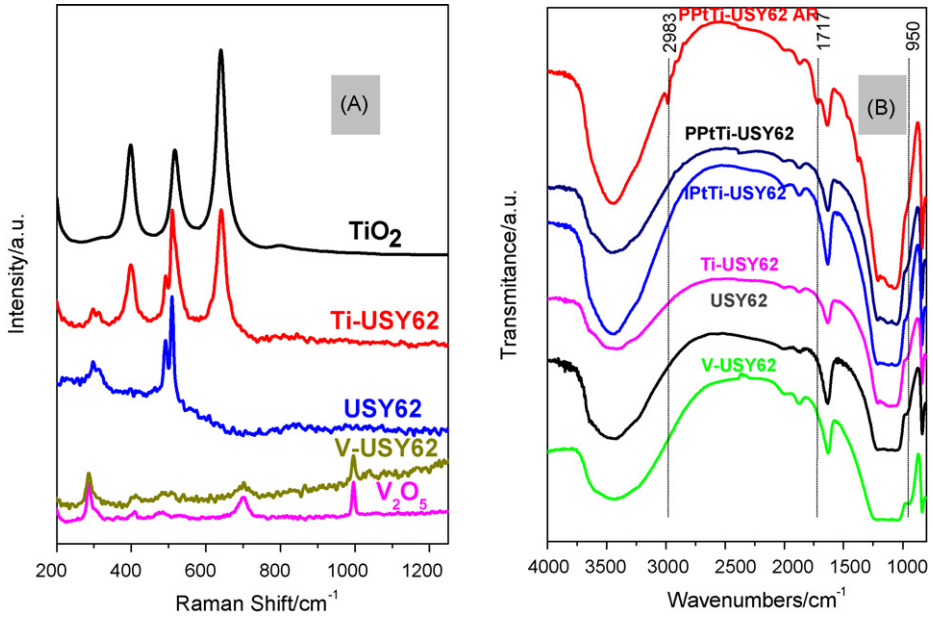

Fig. 3. Raman (A) and FT-IR (B) spectra of some of the systems synthesized in the present work. The suffix "AR" stands for "after reaction".

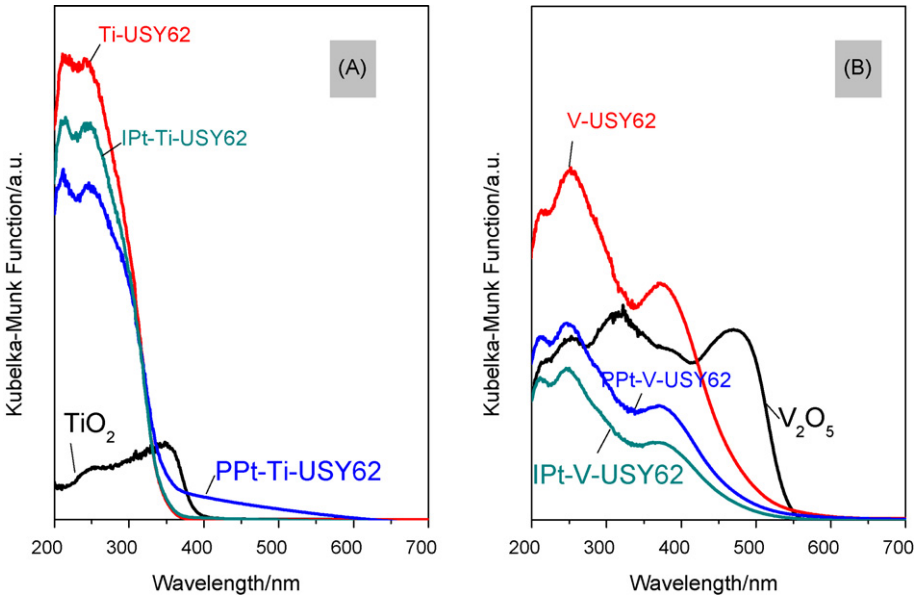

Fig. 4. UV–vis spectra of some titanium-based (A) or vanadium-based (B) photocatalysts.

spectrum as compared to bulk titania. Such a shift to the shorter wavelength in the absorption band of titanium oxides can be attributed to the size quantization effect due to the presence of Ti-oxide particles smaller than 10 nm [25,26] and could account for the high photocatalytic activity of Ti-USY62.

As regards V-USY62, its XRD spectrum is represented in Fig. 2. In a similar way as described for Ti-USY62, no bands corresponding to V_2O_5 are observed, which again suggest that if present such an oxide has a low crystallite size. As far as pure V_2O_5 is concerned, its crystallite size as determined from 0 0 1 reflection at ca. $2\Theta = 20.29^\circ$, was 83 nm. Raman spectroscopy of V-USY62 (Fig. 3A) shows bands at 285, 993 and 699 cm^{-1} which confirms the presence of crystalline V_2O_5 [27,28]. No band at 1039 cm^{-1}, corresponding to stretching vibration of terminal V=O bonds in monomeric, tetrahedral vanadia surface species with three bonds to the support surface ($(SiO)_3$ V=O) is observed [27]. This finding, together with the no change in the 950–960 cm^{-1} region (attributed to Si–O–V stretching vibration) in V-USY62 [29,30] as compared to USY62, suggest that vanadium has not been incorporated into the zeolitic structure. UV–vis spectra of V-USY62 (Fig. 4B) is blue-shifted as compared to that of V_2O_5 thus suggesting a lower crystallite size in the former.

3.2. Platinum and silver containing zeolites

As mentioned above, Ti-USY62 and V-USY62 were selected for incorporation of Ag and Pt by the impregnation and photodeposition method. Some features concerning their characterization are summarized in Table 1.

On the one hand, incorporation of silver by both methods is almost quantitative as shown by the Ag/Ti atomic ratio percentage being close to 10% (see entries 16 and 17 in Table 1). It is well-known than Ag^+ can easily be photoreduced, reduction probably favored by the solvent, propan-2-ol, which could account for its easy incorporation into zeolites. Leaching of vanadium could explain the high experimental Ag/V percentage (over 30% for both PAg-V-USY62 and IAg-V-USY62, entries 18 and 19, respectively).

On the other hand, platinum incorporation through photodeposition is more difficult than that of silver, as expected from the corresponding redox potentials ($Pt^{2+}/Pt = +1.2$ eV whereas $Ag^+/Ag = 0.80$ eV) [31]. Moreover, Pt^0 is less prone to leaching than Pt^{n+} which could explain the higher Pt/(Ti or V) atomic percentage obtained through photodeposition as compared to impregnation method (compare entries 12–13 and 14–15 in Table 1).

Results obtained for gas-phase photocatalytic selective oxidation of propan-2-ol are given in Fig. 5. For the sake of comparison, those achieved with USY62, Ti-USY62 and V-USY62 have also been included.

From Fig. 5A and B it is clear that under our experimental conditions incorporation of platinum into the systems results in an increase in molar conversion of both Ti-USY62 and V-USY62 systems. On the other hand, silver has a detrimental effect on activity. When both impregnation and photodeposition methods are considered, the latter leads to more active systems, less deactivated during the 5 h on stream and which additionally exhibit higher selectivities to acetone.

Therefore, photodeposition of Pt on Ti-USY62 resulted in initial molar conversion increasing from 46.7% up to 71.1%, whereas deactivation after 5 h dropped from 33.8% to only 2.5%. Moreover, selectivity to acetone after a time-on-stream of 5 h for PPt-Ti-USY62 was 90%.

It is interesting to point out that platinum weight percentage in PPt-Ti-USY62 is 0.71% whereas for IPt-Ti-USY62 it is only 0.04% which explains the catalytic behavior of the latter being similar to that of Ti-USY62.

Vanadium-containing systems present the same tendency as described for Ti-ones though they are comparatively less active. PPt-V-USY62 exhibit 45.6% molar conversion of propan-2-ol after 5 h whereas such a chemical is only transformed in a

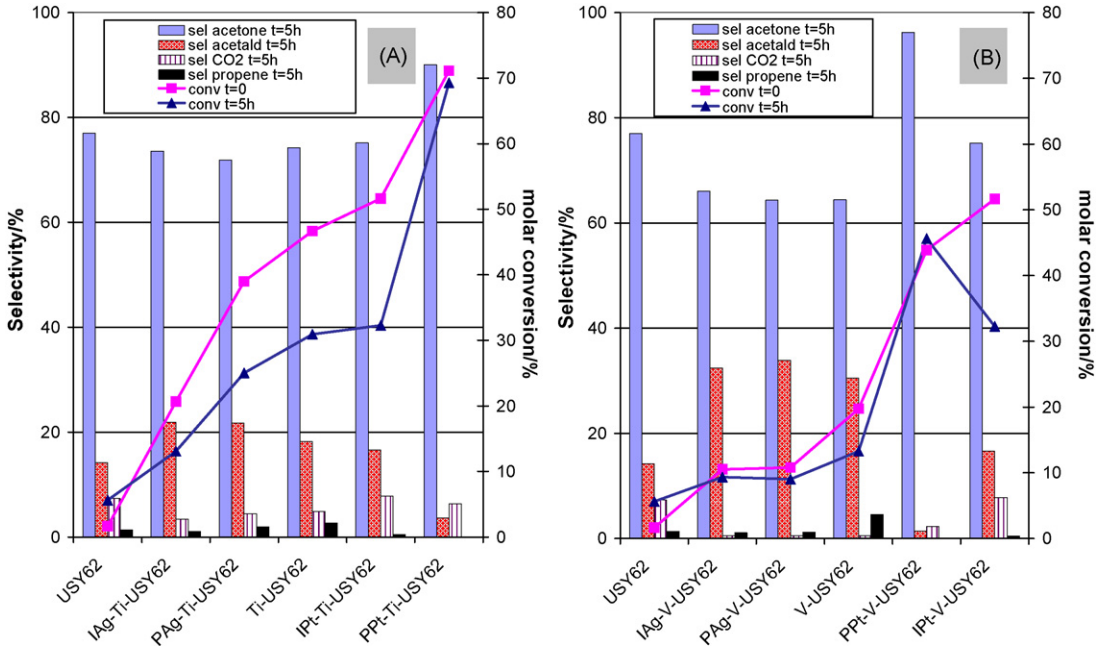

Fig. 5. Results obtained for the gas-phase selective photooxidation of propan-2-ol with the vanadium and titanium-based systems synthesized in the present work before and after incorporation of silver or platinum. For the sake of comparison, results achieved with USY62 have also been included.

13.3% with V-USY62. It is noteworthy that the highest selectivity to acetone within the zeolitic systems studied in the present work is obtained with PPt-V-USY62. Such a system does not seem to deactivate after 5 h but instead molar conversion slightly increases from 43.9% ($t = 0$ h) to 45.6% ($t = 5$ h) whereas final selectivity to acetone is 96.2% as compared to 64.4% for V-USY62. Interestingly, such spectacular improvement was achieved with a platinum weight percentage of only 0.11% (see Table 1, entry 14).

FT-IR spectra of all the Ti- and V-containing systems used in the present piece of research for a time-on-stream of 5 h were performed. All systems show some bands at ca. 2983, 1458 and 1378 cm^{-1} which could be assigned to ν(C–H), $\delta_{as}(CH_3)$ and $\delta_s(CH_3)$, respectively, of isopropoxide species [32]. In the case of PPt-Ti-USY62 an additional band at ca. 1717 cm^{-1} is observed. Comparison with the spectrum of pure acetone allowed us to assign such a band to its ν(C=O). The same band, though much less intense is only observed for IPt-Ti-USY62. Therefore, it could be attributed to any kind of interaction of acetone with platinum which could also be related to the high selectivity to such a chemical exhibited by PPt-Ti-USY62.

Finally, different experiments were performed on the PPt-Ti-USY62 system in order to rule out the possibility of thermal activity (Fig. 6). After 15 h of reaction without any deactivation, switching off the lamp (1) results in a dramatic decrease in molar conversion whereas initial conversion is rapidly recovered on switching the lamp on (2). If light intensity is adjusted to 82% of the total (3), conversion drops to similar values (4) to those obtained using a heat ray cutting filter (Hamamatsu Re: A7028-03, cut wave length 400–700 nm) whose placing results in UV transmittance dropping from 1.1 to 0.9 W cm^{-2} (18% decrease). Moreover, propan-2-ol transformation conducted in another reactor under similar conditions but thermally, resulted in high selectivities (close to 90%) to propene + diisopropyl ether over the range 125–425 °C, acetone being a minor product. Therefore, no significant thermal effect is observed under our experimental conditions and, consequently, photocatalytic activity is to account for propan-2-ol transformation.

Pichat et al. [33] studied the consequence of platinum doping of anatase on photoassisted reactions concluding that below a certain platinum content, the metal reduces the charge recombination in TiO_2 whereas above such a value recombination at the metal particles progressively cancels such a beneficial effect. In our case, platinum content in PPt-Ti-USY62 (0.71%) seems to be low enough as to have a beneficial effect on photoactivity whereas the high silver content in all the systems (above 1.5%) seems to favor electron–hole recombination.

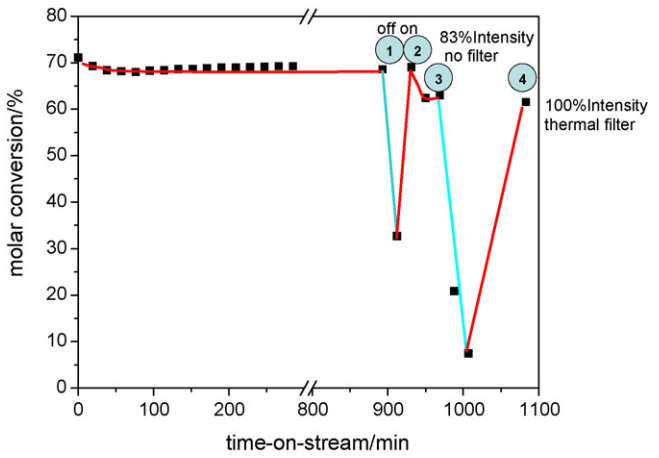

Fig. 6. Different tests carried out to evidence the negligible thermal effect in gas-phase selective photooxidation of propan-2-ol on PPt-Ti-USY62.

4. Conclusions

The above-mentioned results allow us to draw the following conclusions:

The sol–gel synthesis of titania and vanadia on USY zeolites led to an improvement in photocatalytic activity for gas-phase photoselective oxidation of propan-2-ol. XRD, Raman and FT-IR spectroscopies allowed us to conclude that the systems were constituted by titania (anatase) or vanadia particles with a lower crystal size than the corresponding pure TiO_2 and V_2O_5 systems. The decrease of crystal size is probably to account for the observed blue-shift in UV–vis spectra of zeolites and the better photocatalytic performance.

Platinum and silver were subsequently incorporated to the most-active systems by photodeposition and impregnation, the former method being more effective under our synthetic conditions.

Incorporation of platinum results in a significant increase in molar conversion whereas the presence of silver is detrimental to activity. A small content in metal (case of platinum with weight percentage of 0.71% and 0.11% for PPt-Ti-USY62 and PPt-V-USY62, respectively) could retard electron–hole recombination, thus improving photoactivity. On the other hand, higher contents in metal (case of silver with over 1.5% by weight) could be detrimental to activity as the result of the metal acting as electron–hole recombination center. Photodeposited platinum systems show a very low deactivation and very high selectivity to acetone (ca. 90% and 96% for PPt-Ti-USY62 and PPT-V-USY62, respectively). The effect of platinum thermal activity was found to be negligible.

In conclusion, very active, highly selective and poorly deactivated catalysts for gas-phase selective photoxidation of propan-2-ol to acetone were obtained through the sol–gel synthesis of titania and vanadia on USY zeolites and subsequent platinum photodeposition.

Acknowledgments

The authors gratefully acknowledge the financial support from Ministerio de Educación y Ciencia (Project CTQ-2005-04080/BQU) and Junta de Andalucía (Project FQM 191) both co-funded with FEDER.

References

[1] J.M. Herrmann, Catal. Today 53 (1999) 115.
[2] P. Pichat, in: M.A. Tarr (Ed.), Chemical Degradation Methods for Wastes and Pollutants: Environmental and Industrial Applications, Marcel Dekker Inc., New York, Basel, 2003, pp. 77–119.
[3] P. Fernández, J. Blanco, C. Sichel, S. Malato, Catal. Today 101 (2005) 345.
[4] P. Calza, C. Paze, E. Pelizzetti, A. Zecchina, Chem. Commun. (2001) 2130.
[5] Y. Paz, C.R. Chimie 9 (2006) 774.
[6] Y. Sagatelian, D. Sharabi, Y. Paz, J. Photochem. Photobiol. A 174 (2005) 253.
[7] A. Sclafani, M.N. Mozzanega, J.-M. Herrmann, J. Catal. 168 (1997) 117.
[8] C.-P. Chang, J.-N. Chen, M.-C. Lu, J. Chem. Technol. Biotechnol. 79 (2004) 1293.
[9] U.R. Pillai, E. Sahle-Demessie, J. Catal. 211 (2002) 434.
[10] A. Corma, H. García, Chem. Commun. (2004) 1443.
[11] G. Cosa, M.S. Galletero, L. Fernández, F. Márquez, H. García, J.C. Scaiano, New J. Chem. 26 (2002) 1448.
[12] S. Anandan, M. Yoon, J. Photochem. Photobiol. C 4 (2003) 5.
[13] K. Hashimoto, K. Wasada, M. Osaki, E. Shono, K. Adachi, N. Toukai, H. Kominami, Y. Kera, Appl. Catal. B 30 (2001) 429.
[14] H. Yahiro, T. Miyamoto, N. Watanabe, H. Yamaura, Catal. Today 120 (2007) 158.
[15] M.A. Aramendía, A. Marinas, J.M. Marinas, J.M. Moreno, F.J. Urbano, Catal. Today 101 (2005) 187.
[16] S.A. Johnson, E.S. Brigham, P.J. Ollivier, T.E. Mallouk, Chem. Mater. 9 (1997) 2448.
[17] S. Sakthivel, H. Kisch, Angew. Chem. Intern. Ed. 42 (2003) 4908.
[18] J.E. Herrera, D.E. Resasco, J. Phys. Chem. B 107 (2003) 3738.
[19] Y. Miyake, H. Tada, J. Chem. Eng. Jpn. 37 (2004) 630.
[20] J.C. Colmenares, M.A. Aramendía, A. Marinas, J.M. Marinas, F.J. Urbano, Appl. Catal. A 306 (2006) 120.
[21] W. Xu, D. Raftery, J. Phys. Chem. B 105 (2001) 4343.
[22] W.X. Zhang, C.B. Wang, H.L. Lien, Catal. Today 40 (1998) 387.
[23] M. Kang, W.-J. Hong, M.-S. Park, Appl. Catal. B 53 (2004) 195.
[24] S.V. Awate, N.E. Jacob, S.S. Deshpande, T.R. Gaydhankar, A.A. Belhekar, J. Mol. Catal. A 226 (2005) 149.
[25] M. Anpo, M. Takeuchi, J. Catal. 216 (2003) 505.
[26] N. Jagtap, V. Ramaswamy, Appl. Clay Sci. 33 (2006) 89.
[27] M. Baltes, K. Cassiers, P. Van Der Voort, B.M. Weckhuysen, R.A. Schoonheydt, E.F. Vansant, J. Catal. 197 (2001) 160.
[28] S. Besselmann, E. Loffler, M. Muhler, J. Mol. Catal. A 162 (2000) 401.
[29] V. Murgia, E.M. Farfán Torres, J.C. Gottifredi, E.L. Sham, Appl. Catal. A 312 (2006) 134.
[30] M.D. Wildberger, T. Mallat, U. Göbel, A. Baiker, Appl. Catal. A 168 (1998) 69.
[31] Information available at www.kft-split.hr/periodni/fr/abc/ems.html.
[32] J. Araña, J.M. Doña Rodríguez, O. González Díaz, J.A. Herrera Melián, J. Pérez Peña, Appl. Surf. Sci. 252 (2006) 8193.
[33] P. Pichat, J.M. Herrmann, J. Disdier, M.N. Mozzanega, H. Courbon, Stud. Surf. Sci. Catal. 19 (1984) 319.